Deflected Thrust Effects on a Close-Coupled Canard Configuration

James L. Thomas,* John W. Paulson Jr.,† and Long P. Yip*
NASA Langley Research Center, Hampton, Va.

The effects of deflected thrust on the stability and performance of a close-coupled canard fighter configuration are presented. These results were obtained at low speeds in the Langley V/STOL tunnel. Transonic as well as low-speed results are also presented for an unpowered close-coupled canard and a supercruiser configuration. The V/STOL tunnel data indicate an increase in maximum lift and reductions in drag due to lift with the addition of two-dimensional vectored thrust at the wing inboard trailing edge. The longitudinal pitchup associated with the unpowered configuration at higher angles of attack was significantly reduced with power.

Nomenclature

C_D = drag coefficient, drag/$q_\infty S$
C_m = pitching-moment coefficient, pitching moment/$q_\infty S\bar{c}$
C_L = lift coefficient, lift/$q_\infty S$
C_T = thrust coefficient, thrust/$q_\infty S$
c = wing or canard chord
$\bar{c}$ = mean aerodynamic chord
e = induced drag efficiency parameter
p_s = excess specific power
q = dynamic pressure
S = wing reference area
V = linear velocity
α = angle of attack, deg
δ = deflection of flap or nozzle, deg
Λ = sweep angle

Subscripts

E = equivalent thrust-removed coefficient
f = flap
j = jet
N = nozzle
0 = minimum
$\perp$ = perpendicular
∞ = freestream

Introduction

EXTENSIVE unpowered studies at the Langley Research Center by B. B. Gloss on a generalized wind-tunnel model have shown increases in maximum lift coefficient with the addition of close-coupled canard/strake combinations to several wing planforms typical of highly maneuverable aircraft.[1,2] These increases are primarily associated with the additional lift developed on the canard and/or strake and the beneficial interaction of the canard/strake on the wing at the higher angles of attack. Analysis of the results in Ref. 3 indicates reductions in drag due to lift for the canard, strake, and wing camber. These benefits, however, are accompanied with a longitudinal instability, or pitchup, at the higher angles of attack because of the vortex lift developed on the forward strakes.

Presented as Paper 77-887 at the AIAA/SAE 13th Propulsion Conference, Orlando, Fla., July 11-13, 1977; submitted Sept. 14, 1977; revision received Dec. 12, 1977.

Index category: Aerodynamics.

*Aerospace Technologist, Low-Speed Aerodynamics Branch. Member AIAA.

†Aerospace Technologist, Low-Speed Aerodynamics Branch.

A larger version of one of the most promising configurations tested by Gloss was fabricated with plain flaps and two-dimensional nozzles at the wing root trailing edge. The model was tested in the Langley V/STOL tunnel at thrust coefficients typical of those available at transonic maneuver conditions.[4] The results indicate increases in maximum lift coefficient and reductions in drag due to lift with deflected power as well as a significant decrease in the pitchup associated with the unpowered configuration. Lift jets were also placed in the nose of the model, and tests were run at thrust coefficients and jet deflection angles similar to those that might be encountered during hover and transition conditions of a VTOL configuration. The results indicate a beneficial induced effect with the deflected thrust positioned at the wing trailing edge. The results from tests of both configurations are discussed further herein.

The models tested had little or no design optimization in that they had no twist, camber, or leading-edge radius. With proper attention to the wing and canard near-field designs, further reductions in drag due to lift could be obtained. Some discussion of the process used to design a model representative of a configuration designed to meet maneuvering requirements at transonic speeds and also high-lift requirements at low speeds is included. Also, some examples of supersonic fighter configurations being considered to meet both maneuvering and high-lift requirements are presented.

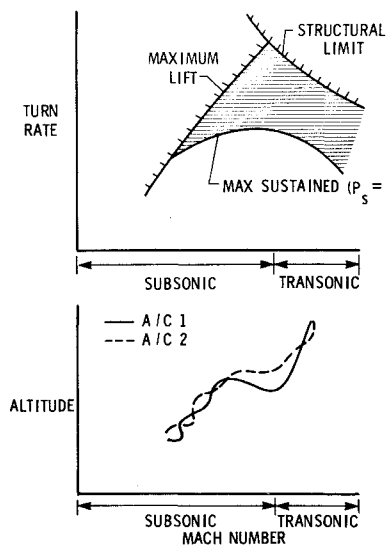

Fig. 1 Maneuver boundaries and typical time history of one-on-one combat.

Low-Speed Performance Studies

The maneuver boundaries for a fighter aircraft are shown schematically in Fig. 1. The instantaneous maneuver limit at subsonic speeds is set by maximum lift and maximum structural loading, while the sustained limit is set by thrust minus drag levels. The instantaneous maneuver limit at supersonic speeds is typically set by structural load limits or thrust limits. Simulation of one-on-one combat in the Langley differential maneuvering simulator with similar aircraft has typically produced time histories of altitude vs Mach number, as shown schematically in Fig. 1. The sustained one-on-one engagement for evenly matched aircraft quickly degenerates to subsonic speeds, while a clearly superior design can end the engagement and still remain near original altitude and speed. It is unlikely that an aircraft would fall to the lower speeds because of increased vulnerability to both ground attack and air attack from more than one aircraft. However, some conditions necessitate an absolute one-on-one engagement and it is for those conditions that the experimental results at low Mach numbers reported herein apply directly.

The degree to which the data obtained at low Mach numbers is applicable to the higher speeds depends on the slenderness of the configuration and the design stage for which data are required. The equivalance theory of Oswatitsch and Keune states that for slender bodies, the flow is governed by a longitudinal potential dependent on the equivalent area distribution and the Mach number and a crossflow potential dependent only on the local cross section and independent of the Mach number. The vortex lift developed on slender configurations is dominated by the crossflow conditions. Therefore, it seems reasonable that planform shaping and interference flowfield studies conducted at low speeds during the preliminary design stage would provide a valuable insight into the lift-dominated flowfields that will be encountered during maneuvering at transonic speeds. The detailed design for desired pressures on the aircraft above the critical Mach number dictates, of course, the use of nonlinear design methods and wind-tunnel testing at the higher design Mach numbers.

The experimental variation of longitudinal aerodynamic characteristics for a supersonic cruise fighter model is shown in Fig. 2.[5] For the slender configuration with highly swept leading edges, the lift and drag are almost invariant up to 0.9 Mach number. The pitching-moment data show the most variation with Mach number, indicating a more nose-down moment at the higher Mach numbers. The variation of lift, drag, and moment for a close-coupled wing-canard model is shown in Fig. 3.[1,6] The wing is approaching the limit to which the slenderness criterion can be applied, but the canard interference promotes vortex lift on the wing so that the entire configuration is a vortex lift-dominated flowfield. Again, the lift and drag are almost invariant with Mach number, while the moment shows a more nose-down trend with Mach number. Variation of the incremental lift, drag, and pitching moment due to the addition of the canard with Mach number is shown in Fig. 4. The interference trends due to canard placement are consistently predicted through the Mach number range demonstrating that low-speed tests can provide a cost effective way of obtaining preliminary aerodynamic trends for configurations with highly three-dimensional lift dominated flowfields.

Test Results for Maneuver Configuration

A three-view drawing and geometric characteristics of the model tested in the Langley V/STOL tunnel are given in Fig. 5 and a photograph of the model installed in the test section is shown in Fig. 6. The model geometry is identical to a model tested by Gloss with the addition of two-dimensional nozzles at the wing root and slightly different canard strakes.[1,2] The model was tested over an angle-of-attack range of -4 deg to 40 deg and a thrust coefficient range up to 0.3.

Longitudinal characteristics of the unpowered configuration are similar to those obtained previously by Gloss and are presented in Fig. 7.[4] The canard and strake provide increments in maximum lift coefficients of 1.0 and 0.2, respectively. The moment center selected provides a longitudinal instability of about 0.06 ($\partial C_m/\partial C_L = 0.06$) with the wing and canard. The pitchup caused by the vortex lift from the strake is clearly seen at the higher angles of attack.

The longitudinal data for the wing-canard configuration with flaps and power ($C_T = 0.2$) is shown in Fig. 8. The addition of power increases the maximum lift coefficient both with and without flaps. With flaps deflected and no power, pitchup ($\partial C_m/\partial C_L = 0.13$) occurs even without the strake due to flow separation over the flaps. The pitchup was eliminated over a large C_L range with the addition of power. The data presented are not trimmed, since the canard tested was fixed

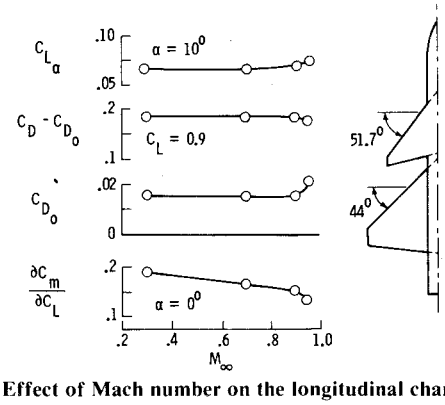

Fig. 3 Effect of Mach number on the longitudinal characteristics of a close-coupled canard wing model.

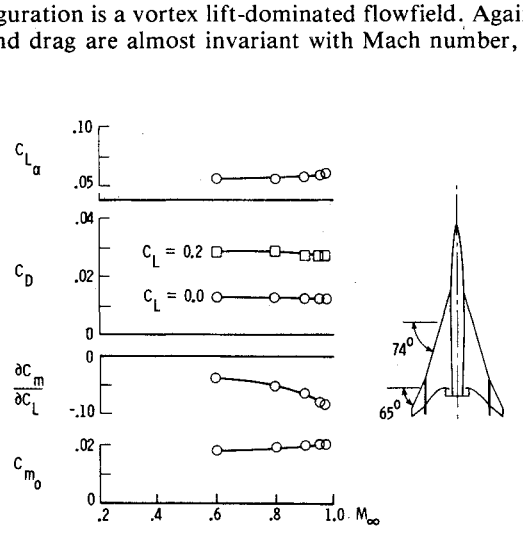

Fig. 2 Effect of Mach number on the longitudinal characteristics of a supersonic cruise fighter model.

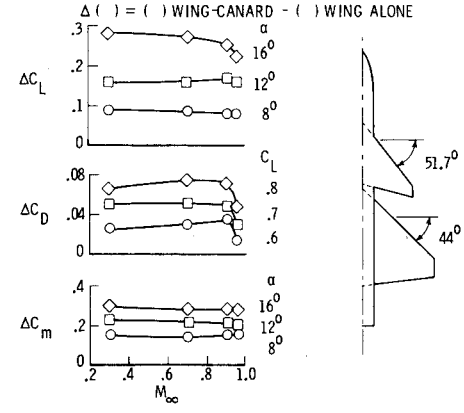

Fig. 4 Effect of Mach number on incremental lift, drag, and pitching moment due to addition of canard.

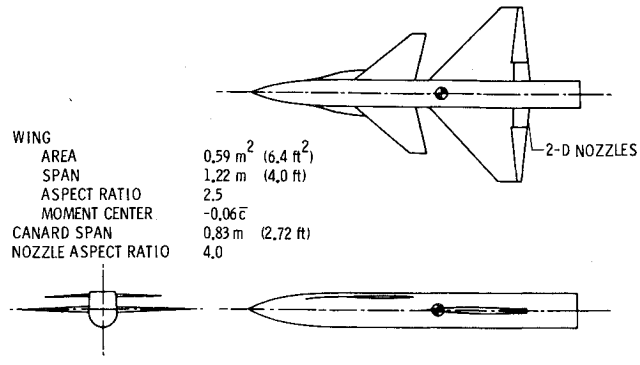

Fig. 5 Three-view sketch of close-coupled canard/strake fighter configuration tested in the Langley V/STOL tunnel.

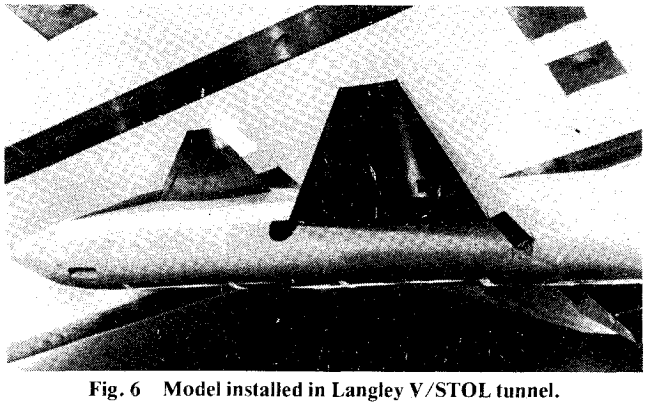

Fig. 6 Model installed in Langley V/STOL tunnel.

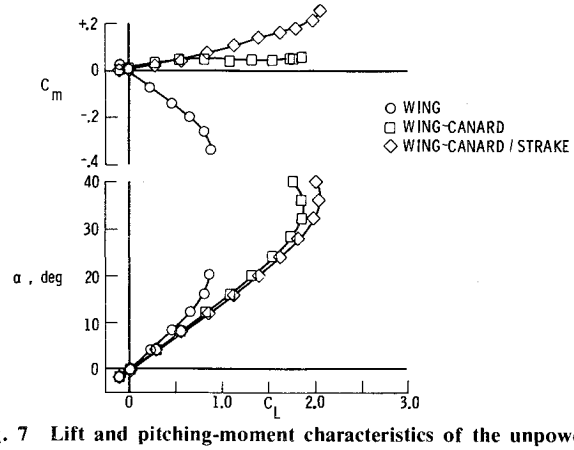

Fig. 7 Lift and pitching-moment characteristics of the unpowered wing-canard/strake configuration.

in incidence and is presented to show the trends and magnitudes of deflected thrust effects. The high loads necessary on the canard for trim dictate an improved section design with both leading- and trailing-edge devices.

Since the thrust coefficients available at typical maneuver conditions are small, the lift obtained from the thrust component in the lift direction or from induced circulation is small. The vectored-thrust provides increased lift from the boundary-layer control over the lifting surfaces. The effects of flaps and power on the wing-canard configuration with the direct thrust component removed from the lift and moment is shown in Fig. 9. This demonstrates that the increase in maximum lift coefficient and reduction in pitchup is largely attributed to the boundary-layer control over the wing and trailing-edge flaps.

The longitudinal characteristics of the wing-canard/strake configuration are shown in Fig. 10. At the higher lift coefficient, there is a more severe pitchup than without the

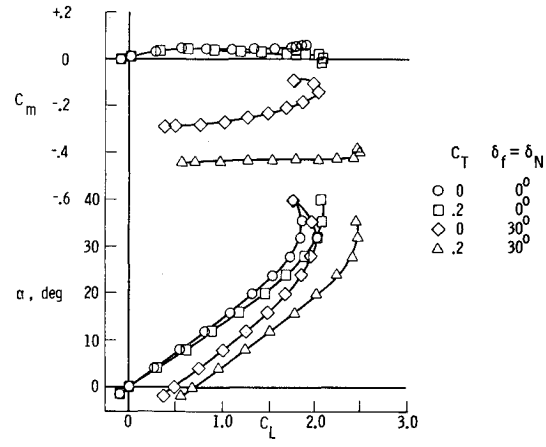

Fig. 8 Effects of flap deflection and power on the lift and pitching moment of the wing-canard configuration.

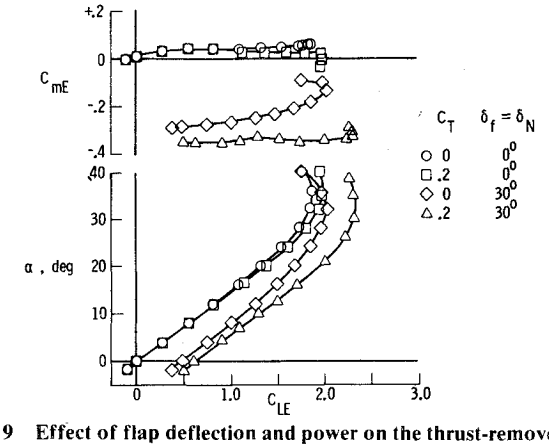

Fig. 9 Effect of flap deflection and power on the thrust-removed lift and pitching moment of the wing-canard configuration.

strakes, especially for $\delta_f = 30$ deg where $\partial C_m/\partial C_L = 0.30$ at $\alpha = 20$ deg to 25 deg. The effect of the power was to reduce the pitch instability to $\partial C_m/\partial C_L = 0.11$ at $\alpha = 20$ deg to 25 deg. The increments in maximum lift obtained with flaps and power are similar to those without the strakes.

Previous analyses have shown the reductions in drag due to lift when the canard and strakes are added to the wing. The effect of power and flaps is to further reduce the drag due to lift (C_{D_i}) as shown in Fig. 11. The term

$$\left(\frac{\Delta C_{D_i}}{C_L{}^2}\right)_{\text{aero}} = \frac{C_D - C_{D_0} + C_T\cos(\alpha+\delta)}{[C_L - C_T\sin(\alpha+\delta)]^2}$$

is an experimental thrust-removed drag due to lift parameter $(\Delta C_{D_i}/C_L{}^2)_{\text{aero}}$ commonly expressed as $1/\pi Ae$ for unpowered models (Ref. 3). The theoretical minimum was calculated from a far-field drag optimization technique.[3] Although reductions in drag due to lift occurred with power, none of the curves reached the theoretical minimum largely because both the wing and canard were uncambered with sharp leading edges.

Test Results for VTOL Configuration

The canard-wing configuration was also tested at larger thrust coefficients (up to $C_T = 5$) and flap deflection angles representative of the hover and transition conditions of a VTOL configuration. Lift jets exiting from two elliptically shaped slots were located in the nose of the model. The forward jets provided approximately one-third of the total thrust and were located forward to trim the large nose-down moments from the trailing-edge jets. Results from the tests at $\alpha = 0$ deg and deflection angles on the nozzle and flap equal to

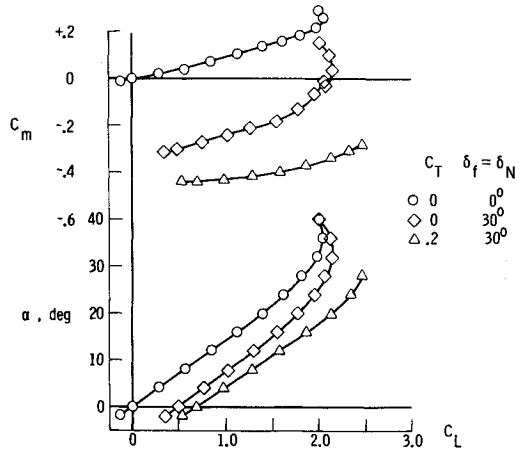

Fig. 10 Effect of flap deflection and power on the lift and pitching moment of the wing-canard/strake configuration.

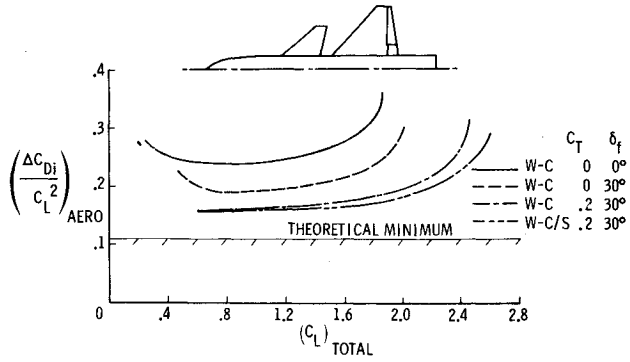

Fig. 11 Effect of flap deflection and power on the thrust-removed drag due to lift variation with total lift coefficient.

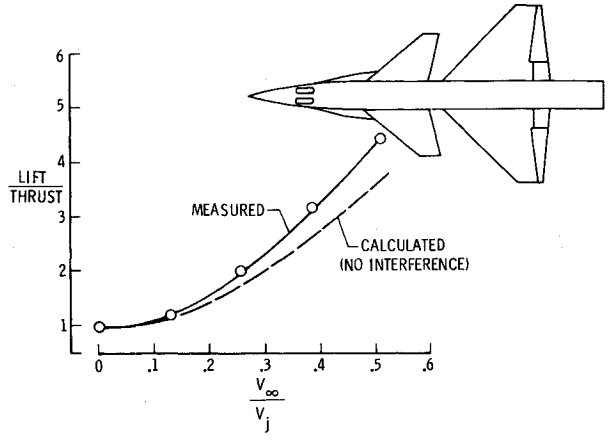

Fig. 12 Interference effects on close-coupled canard VTOL configuration.

90 deg and 60 deg, respectively, are shown in Fig. 12. The rearward placement of the nozzles on the wing induces a beneficial effect via circulation so that the measured lift is greater than that predicted by adding the lift of the jet and wing-canard tested separately. The forward jet produces suction pressures on the fuselage and wing-canard lower surfaces, which cause a loss in lift. The elliptically shaped slot jets were selected based on previous results which indicated that this shape reduces adverse lift interference.[7]

Results from previous wind-tunnel studies at similar conditions of a model similar to the Harrier are shown in Fig. 13.[8] The high pressures induced on the wing from the jets exhausting ahead of and at the wing cause a detrimental

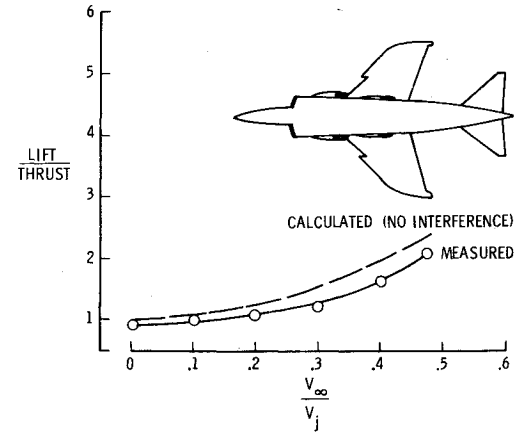

Fig. 13 Interference effects on Harrier configuration.

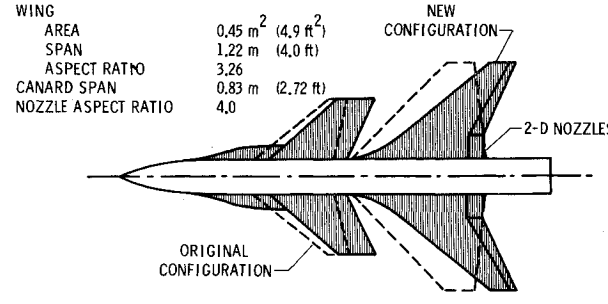

Fig. 14 New close-coupled wing/canard configuration.

interference. The measured lift is less than that predicted assuming no interference.

Follow-On Studies

A sketch of a new research close-coupled canard wing configuration to be tested in the Langley V/STOL tunnel later this year is shown in Fig. 14. The configuration was designed to minimize compressible and viscous effects at high lift. It is intended to be representative of a realistic transonic maneuvering configuration. The model was constrained to have the same fuselage and powered nozzles as the original configuration. The wing leading- and trailing-edge sweeps were increased ($\Lambda_{c/2} = 40$ deg) to reduce nonlinear compressibility effects and also to move the aerodynamic center rearward so that the nose-down moments due to the jet are reduced for a given level of stability. A glove was added inboard on the wing in an attempt to sweep the isobars forward and give a more two-dimensional-type loading outboard. The canard has the same leading- and trailing-edge sweeps as the wing. The canard taper ratio was selected so that a reasonable tip chord existed when the canard span was increased (with bolt-on additions) to that of the wing. This variable geometry was built into the model so that the effect of canard span to wing span on induced drag can be determined experimentally.

The wing and canard twist, camber, and thickness were determined as shown in Figs. 15 and 16. Basically, a supercritical airfoil section known to have good two-dimensional viscous and compressibility characteristics at transonic speeds was modified for three-dimensional induced effects. Using the Korn-Garabedian program, a design curve of section-lift coefficient (C_l) vs drag divergence Mach number (M_{DD}) was developed for scaled versions of the original airfoil (see Fig. 15).[9] Using the nonplanar unified vortex-lattice theory of Ref. 10, the sweep of the chordwise center of pressure, $(x/c)_{c.p.}$, was calculated at the design Mach number of 0.9. Using the infinite swept-wing analogy ($C_{l_\infty} = C_{l_\perp} \cos^2\Lambda$) and the two-dimensional drag divergence plot, the variations of maximum freestream section lift coefficients on the wing and

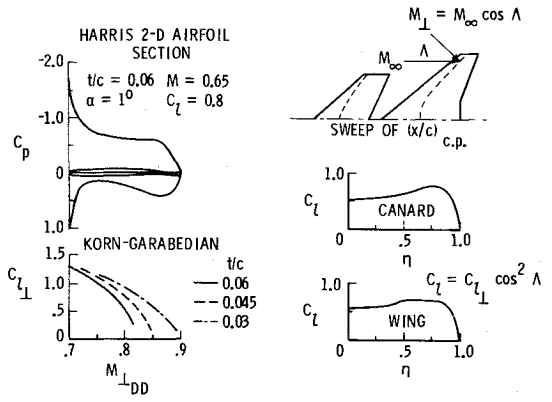

Fig. 15 Variation of maximum section-lift coefficients based on drag divergence.

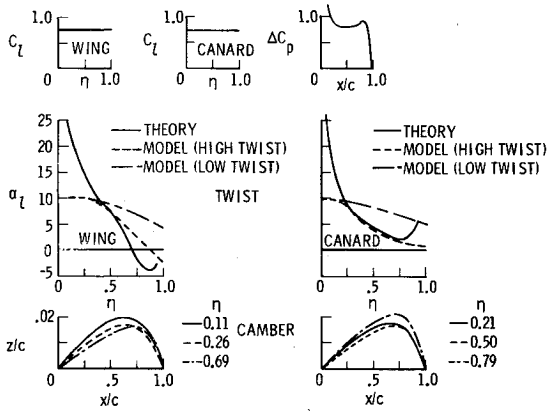

Fig. 16 Twist and camber based on constant freestream section-lift coefficient and desired two-dimensional chordwise loading.

canard that can be realized, while staying below drag-divergence Mach number, were generated.

An inverse program was used to calculate the twist and cambers required on the planform. The local freestream section lift was chosen as the maximum from Fig. 15 and held constant across the span, realizing that the resulting twists would have to be modified in the root and tip regions. The chordwise loading was chosen as the two-dimensional subcritical loading of the original section. The resulting twists and cambers are shown in Fig. 16. The twists were fitted approximately to the theoretical distributions as shown by the dashed lines. Relying on structural deflections to provide partial twist at high maneuver load conditions, two versions of the research model, identical except for the levels of twist, are being fabricated. The low-twist version will be used to study conventional takeoff and landing high-lift performance and the high-twist version high-angle-of-attack maneuver performance. Both versions will have full-span variable leading- and trailing-edge devices on both the wing and canard. The canard incidence will be variable so that trimmed high-lift levels can be obtained at both high-angle-of-attack (low-thrust) and low-angle-of-attack (high-thrust) conditions. This design procedure was not intended to produce an optimum transonic design. Rather, it was intended to develop a configuration that would be realistic of that required for transonic maneuvering conditions.

Follow-on designs being considered for a supersonic configuration with design Mach number of 1.8 are shown in Fig. 17. For these configurations, the intent will be to aerodynamically design the model to be representative of that required for efficient supersonic cruise. However, it will be tested at low speeds in takeoff and landing and at high angles of attack. Two possible configurations are shown that may give good takeoff, landing, and maneuvering characteristics.

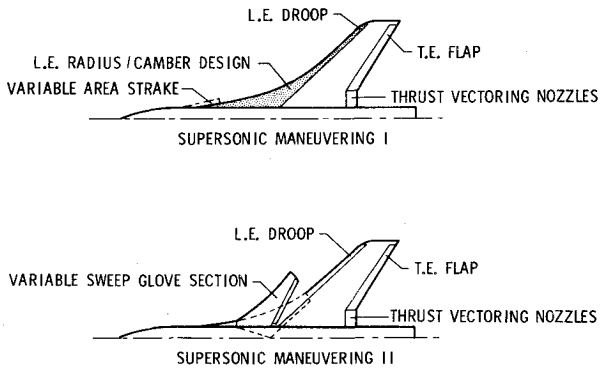

Fig. 17 Conceptual design of supersonic maneuver configuration.

One has a fixed glove with increasing leading-edge radius inboard in addition to camber in order to provide a combination of planform, camber, and thickness blending to relieve leading-edge pressure gradients and thus delay the formation of the leading-edge vortex to higher angles of attack. A variable-area strake is used as pitch control and to initiate vortex-type flow past the angle of attack where the wing can no longer support attached flow. The other concept uses a variable-sweep glove with leading- and trailing-edge devices to provide for trim of the wing trailing-edge flap and vectored-thrust moments. Both concepts would use vectored thrust as in the transonic design. The design goal of both is to provide high lift at high angles of attack with desired levels of stability and sufficient control power to trim the configuration.

Conclusions

Previous results have shown increases in maximum lift and reductions in drag due to lift for close-coupled canard wing configurations. Further increases in maximum lift and reductions in drag due to lift have been demonstrated with power applied through two-dimensional nozzles at the wing trailing edge. Furthermore, the longitudinal instability, or pitchup, was significantly reduced with power. Experimental results for a VTOL configuration show that in the transition mode the rearward nozzle location produces beneficial interactions via induced circulation.

An effort to design a new model with planform, twist, and section shape realistic of a transonic maneuvering configuration has been completed. The new configuration will be tested at low speeds in the Langley V/STOL tunnel to study takeoff, landing, and high-angle-of-attack aerodynamics with power. Some conceptual design for a supersonic configuration having improved high-lift and maneuver characteristics at low speeds are presently being studied.

References

[1]Gloss, B. B., "Effect of Wing Planform and Canard Location and Geometry on the Longitudinal Aerodynamic Characteristics of a Close-Coupled Canard Wing Model at Subsonic Speeds," NASA TN D-7910, 1975.

[2]Gloss, B. B., "The Effect of Canard Leading-Edge Sweep and Dihedral Angle on the Longitudinal and Lateral Aerodynamic Characteristics of a Close-Coupled Canard-Wing Configuration," NASA TN D-7814, 1974.

[3]Tulinius, J. R. and Margason, R. J., "Aircraft Aerodynamics Design and Evaluation Methods," AIAA Paper 76-15, Washington D. C.,1976.

[4]Paulson, J. P., Thomas, J. L., and Yip, L. P., "Low-Speed Power Effects on Advanced Fighter Configurations with Two-Dimensional Deflected Thrust," NASA TM X-74010, 1977.

[5]Morris, O. A., "Subsonic and Supersonic Aerodynamic Characteristics of a Supersonic-Cruise Fighter Model with a Twisted and Cambered Wing Having 74° Sweep," NASA TM X-3530, 1977.

[6]Gloss, B. B., "Effect of Canard Location and Size on Canard-Wing Interference and Aerodynamic-Center Shift Related to

Maneuvering Aircraft at Transonic Speeds," NASA TN D-7505, 1974.

[7]Vogler, R. D. and Goodson, K. W., "Low-Speed Aerodynamic Characteristics of a Fuselage Model with Various Arrangements of Elongated Lift Jets," NASA TN D-7299, 1973.

[8]Margason, R. J., Vogler, R. D., and Winston, M. M., "Wind-Tunnel Investigation at Low Speeds of a Model of the Kestrel (XV-6A) Vectored Thrust V/STOL Aircraft," NASA TN D-6286, 1972.

[9]Bauer, F., Garabedian, P., Korn, D., and Jameson, A., "Supercritical Wing Sections II," *Lecture Notes in Economics and Mathematic Systems*, edited by M. Beckman and H. P. Künzi, Springer-Verlag, New York, 1975.

[10]Tulinius, J., "Unified Subsonic, Transonic, and Supersonic NAR Vortex Lattice," Rockwell International, Downey, Calif., TFD-72-523, 1972.